Journal Name

COMMUNICATION

Mesoporous Polyoxometalate Cluster–Crosslinked Organosilica Frameworks Delivering Exceptionally High Photocatalytic Activity

Eirini D. Koutsouroubi, Alexandra K. Xylouri and Gerasimos S. Armatas*

Mesoporous framework materials comprising lacunary $[SiW_{11}O_{39}]^{8-}$ polyoxometalate clusters covalently connected by ethane-bridged silsesquioxane linkers were synthesized through a block copolymer-templated cross-linking polymerization of 1,2-bis(triethoxysilyl)ethane in acid solution. These new hybrid materials, which exhibit a high density of catalytic sites, large pore surface and ordered pore structure, shown to be highly effective in photocatalytic oxidation of aryl alcohols with molecular oxygen.

Polyoxometalate (POM) clusters, *i.e.* metal-oxygen anionic compounds of the early transition metals (usually of V^V, Mo^{VI}, and W^{VI}), have attracted tremendous attention in the last decade due to their fascinating electrochemical properties and unprecedented molecular and compositional diversity.[1] The ability to preserve the molecular structure against oxidative and hydrolytic decomposition and undergo reversible multielectron transformations offer interesting perspectives for applications of these nanomaterials as catalysts, analytical reagents, multilevel memories and electrochromic and electrochemical devices.[2] However, for technological processes involving transport-related phenomena such as catalysis, it would be highly desirable to integrate POMs into three-dimensional (3D) porous architectures. In principle, this could induce complementary functionalities such as high surface area and catalytic activity, derived from starting components.[3]

The organic-mediated cross-linking polymerization of POMs into 3D porous structures is an appealing method for targeting novel materials with functionality.[4] This approach utilized supramolecular assembly of POM anions with organic linkers (like 1,2,4-triazoles[5] and polycarboxylates[6]), ligand-supported transition-metal bridges[7] or rare earth cations (Ln^{3+})[8] to form open-framework molecular materials. More importantly in these hybrid polymers, the POMs not only can maintain their structural integrity, but also impart their intrinsic physical properties to the framework. Also the organic components playing an important role and can dramatically influence the chemical properties of the former.[9] However, despite the great progress made in this area, the porous structure of these solids is limited by micropore channels (pore size < 2 nm), which in most cases are not fully accessible to guest molecules.[6,10] Recently,

coordinative coupling reactions of Zn-substituted POM, $[ZnWZn_2(H_2O)_2(ZnW_9O_{34})_2]^{12-}$, with various electrophilic linkers (e.g. branched tripodal polyammonium cations) have been realized to produce amorphous mesoporous POM-organic conjugated polymers.[11] Even though these materials possess solvent-accessible pore volume, they have disordered pore structure with moderate Brunauer–Emmett–Teller (BET) surface area (less than 50 m^2g^{-1}). Open-pore POM-organic frameworks with large internal surface area and uniform pores are not obvious, in part because of the poor processability of POMs to create mesoscopic forms, the difficulty in removing the templates inside the pores and the instability of POM structure during synthesis.

Herein, we describe the first reliable synthesis of hybrid mesoporous POM-based organosilicas using a surfactant-assisted co-polymerization of organically-modified $[SiW_{11}O_{39}\{O(SiC_2H_4Si(OH)_3)_2\}]^{4-}$ ($[SiW_{11}(SiOH)_2]^{4-}$, Fig. 1a) building blocks, with ethane-bridged silsesquioxane (1,2-bis(triethoxysilyl) ethane, BTSE) linkers. The approach we report, although is based on the synthesis of periodic mesoporous organosilicas (PMOs)[12], represents a significant extension to previous synthetic routes to isolate porous molecular-framework systems with unique functionality. In a typical preparation, an aqueous acidic solution of BTSE monomers was mixed with $(EO)_{20}(PO)_{70}(EO)_{20}$ (EO: ethylene oxide, PO: propylene oxide) triblock copolymer (P123) template dissolved in water to form clear solution. To this solution was added the $(NMe_4)_4SiW_{11}(SiOH)_2$ POM compound in DMSO and the mixture was stirred for about 24 h at 40 °C. The molar composition in the synthesis mixture was 0.17 P123 : 1333 H_2O : 5.16 BTSE : n $[SiW_{11}(SiOH)_2]^{4-}$: 2.5 HCl : 70.4 DMSO, where n = 0.033, 0.052 and 0.125. The solution contents were then transferred in a Teflon-lined autoclave and heated at 100 °C for 5 days under static conditions to increase the degree of condensation of silsesquioxanes. The template is finally removed by ethanol extraction to recover mesoporous ethane-silica hybrid frameworks with different loading amount (*x*) of $[SiW_{11}O_{39}]^{n-}$ (SiW_{11}) complexes (labeled as *x%* SiW_{11}/MES, Fig. 1b), *i.e.* ~ 9, 15 and 25% (w/w) as measured by elemental X-ray microanalysis (EDS). For control experiments, mesoporous ethane-silica framework material (MES) was also prepared following a similar procedure. Detailed synthetic procedures are reported in the Supporting Information (ESI†). The elimination of template from as-made materials, containing

surfactant, was verified by thermogravimetric analysis (TGA). TGA results indicated that only a ~5% (w/w) of the surfactant remaining in the pores after washing process (Fig. S1, ESI†). As we will show the mesoporous SiW_{11}/MES polymers, which belong to the metal-organic framework class of materials, possess a 3D covalently bonded network of SiW_{11} units and ethane-bridged silane linkers and exhibit large and accessible pore surface. Surprisingly, although $(NBu_4)_8[SiW_{11}O_{39}]$ catalyst is poorly active under the examined conditions, SiW_{11} units govern the catalytic properties of hybrid mesostructure inducing high catalytic activity for oxidation of aryl alcohols with molecular oxygen.

Small-angle X-ray diffraction (XRD) of template-free samples was used to ascertain that these hybrid materials possess mesoscopic order. The XRD patterns, show a primary diffraction peak at low scattering angles (2θ ~ 0.7–0.85°), which is associated with a d spacing of 10.3, 12.0, 12.1 and 12.5 nm for mesoporous MES and SiW_{11}/MES family containing 9, 15 and 25% (w/w) SiW_{11}, respectively (Fig. 1c). Since the porous structure of these materials is obtained as inverse replica of the same surfactant, the systematic increase in pore-to-pore distance with increasing POM loading is consistent with the integration of POM clusters into the porous framework. A decrease in the intensity of the XRD peak, however, could be associated with a deterioration of the long-range order of hybrid mesostructures. The wide-angle XRD ($2\theta > 10°$) indicated the aperiodic nature of the x% SiW_{11}/MES materials at the atomic scale (see Fig. S2, ESI†). This also suggests a molecular dispersion of SiW_{11} clusters in organosilica matrix.
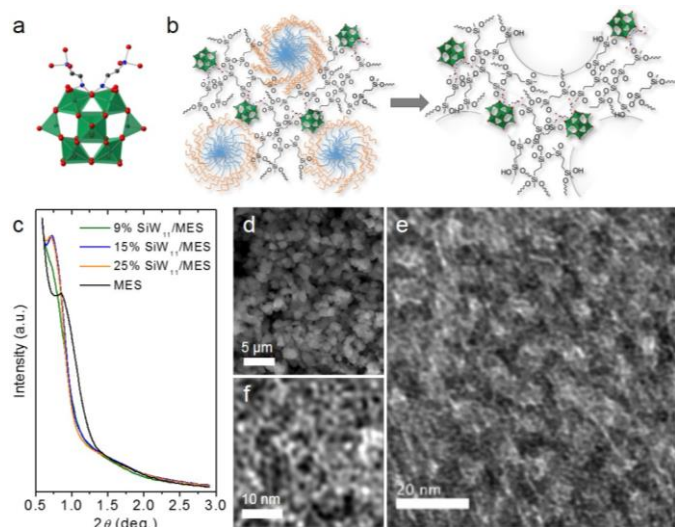

Fig. 1 (a) Molecular structure drawing of the complex $[SiW_{11}O_{39}\{O(SiC_2H_4Si(OH)_3)_2\}]^{4-}$ (O: red, C: black, Si: blue and $\{WO_6\}$: green). (b) Proposed structure of the as-made (containing surfactant) (left) and mesoporous (right) SiW_{11}-containing ethane-silica polymer (SiW_{11}/MES). (c) Small-angle XRD patterns of mesoporous ethane-silica (MES) and x% SiW_{11}/MES materials. (d) Typical SEM image, (e) TEM image, and (f) high-magnification TEM for the mesoporous 15% SiW_{11}/MES sample.

Figs 1d-1f show the morphology of the mesoporous 15% SiW_{11}/MES hybrid prepared by self-assembly process. The SEM micrograph, in Fig. 1d, reveals that the material consists of uniform spherical particles with an average diameter of about 1.1–1.2 μm. According to TEM these particles demonstrate a disordered mesostructure with large uniform mesopores (Fig. 1e). By means of this technique, the pore diameter was estimated to be ~7–8 nm. High-magnification TEM also revealed that SiW_{11} clusters are homogeneously distributed in the pore walls where the high-density POMs appear as discrete dark spots and the polysilsesquioxane

matrix as white area (Fig. 1f). This is consistent with the solid-solution structure found in XRD.

The N_2 adsorption–desorption isotherms of ethanol-extracted samples are shown in Fig. 2a. All isotherms exhibit typical type IV behavior with a combination of H1 and H3 hysteresis loop (according to IUPAC classification), characteristic of mesoporous solids with tubular pore structure.[13] The sharp capillary condensation step at the relative pressures (P/P_0) ~ 0.75–0.85 is associated with narrow mesopore size distribution. The BET surface areas were measured to be 962, 876 and 725 $m^2 g^{-1}$ for 9, 15 and 25% SiW_{11}-loaded SiW_{11}/MES samples respectively, which are slightly lower than that obtained for mesoporous MES (978 $m^2 g^{-1}$, Fig. S3, ESI†). A fit to the isotherms with the NLDFT pore size analysis model gave quite narrow pore size distributions with pore diameters in the range 7.7–7.8 nm (Fig. 2b), in agreement with the TEM images. Table S1 of the ESI† summarizes the textural parameters of the mesoporous pure and SW_{11}-loaded ethane-silica materials.
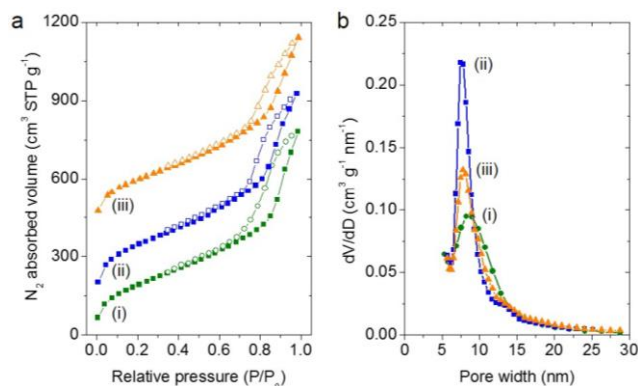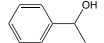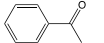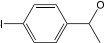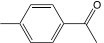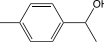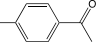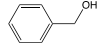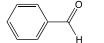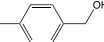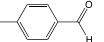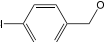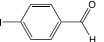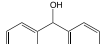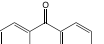

Fig. 2 (a) Nitrogen adsorption-desorption isotherms at 77K and (b) the corresponding NLDFT pore size distributions calculated from the adsorption data for hybrid x% SiW_{11}/MES materials featuring 9% (i), 15% (ii) and 25% (iii) (w/w) SiW_{11} loading. Isotherms are offset along the y axis for clarity.

To probe the molecular structure of the incorporated POM, we utilized infrared (IR) and diffuse reflectance ultraviolet-visible (UV–vis) spectroscopy. The IR spectra of x% SiW_{11}/MES polymers showed the presence of monovacant $[SiW_{11}O_{39}]^{n-}$ clusters by peaks at 530–536 cm^{-1} (ν_s(W–O–W)), 780 cm^{-1} (ν_{as}(W–O–W)) and 914–922 cm^{-1} (ν_{as}(W=O_d)), see Fig. S4 of the ESI†.[14] The spectra also showed the characteristic ν_{as}(Si–O–Si), ν_{as}(Si–O–C) and δ_s(–CH_2–) vibration bands at 1030–1033, 1100–1108 and 1270 cm^{-1}, respectively, of silsesquioxane framework.[15] The UV–vis absorbance spectra of SiW_{11}-loaded polymeric materials display an intense absorption peak at wavelengths 264–268 nm, which is assigned to O(-II)→W(VI) charge-transfer in W–O–W bond of SiW_{11} cluster (Fig. S5, ESI†).[16] Compared to UV–vis spectrum obtained from hybrid $(NMe_4)_4SiW_{11}(SiOH)_2$ complex, these absorptions show a remarkably blue-shift (~10 nm), possible due to the molecular dispersion of POM clusters in the mesoporous matrix. To further determine whether the SiW_{11} units are incorporated intact into the f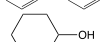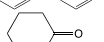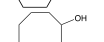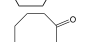ramework, we also performed dissolution of the 15% SiW_{11}/MES structure by immersion in diluted HF solution (5% by weight in water) and the white precipitate, obtained by adding excess of tetrabutylammonium bromide (NBu_4Br) directly to the solution, was identified by X-ray diffraction and Raman spectroscopy. Results from these studies evidenced that the NBu_4^+ precipitate has a similar molecular structure to that of pristine $(NBu_4)_8[SiW_{11}O_{39}]$ compound (Figs S6 and S7, ESI†). Judging from these findings, we suggest that the pore walls of these materials are composed of well-defined Keggin-type $[SiW_{11}O_{39}]^{n-}$ anions connected by ethane-silica struts.

To assess the photocatalytic activity of x% SiW$_{11}$/MES hybrid materials the oxidation of 1-phenylethanol (**1**) into acetophenone (**1a**) was investigated. The results in Table S2 of the ESI† suggest that 15% SiW$_{11}$/MES is the most active catalyst, providing 73% yield of **1a** in 1 h; comparatively 9 and 25% (w/w) SiW$_{11}$-loaded catalysts gave 24% and 57% **1a** yield, respectively, under identical conditions. Also, kinetic analysis on **1** photooxidation evidenced that the initial rate of reaction (k)[17] is greater for 15% SiW$_{11}$/MES compared to the other examined catalyst (Table S2, Fig. S8, ESI†). Of particular note, comparison of hybrid mesostructures to the homogeneous (NBu$_4$)$_8$[SiW$_{11}$O$_{39}$] catalyst, which affords only 5% conv. of **1** in 4 h, indicates that the large porosity and highly spatial distribution of POM clusters on mesoporous surface enhances catalytic activity. Also, the improved activity could result from the unique hydrophobic environment constituted by the ethane functionality of silsesquioxane linkers. Here, the organic constituents may facilitate accumulation of alcohols near the POM active sites through binding effect with phenyl group of substrates. Moreover, the 15% SiW$_{11}$/MES catalyst could be recycled at least three times without obvious loss of the catalytic activity (96 ±2% conv., Fig. S9, ESI†). Notably, no leaching of the SiW$_{11}$ cluster or significant change in the porous structure was observed after catalysis, as evidenced by elemental X-ray microanalysis and N$_2$ physisorption experiments (Fig. S10, ESI†).

Table 1. Aerobic oxidation of various *para*-substituted aryl alcohols by mesoporous 15% SiW$_{11}$/MES catalyst.[a]

	Substrate	Product	Yield (%)[b]	Kinetic constant, k (min^{-1})
1			96	0.020
2			93	0.013
3			94	0.018
4			65[c]	0.017
5			96	0.020
6			97	0.022
7			98	0.038
8			41[d]	0.002
9			46[d]	0.003

[a] Reaction conditions: 0.1 mmol substrate, 3 μmol catalyst (based on SiW$_{11}$ loading), 2 mL α,α,α-trifluorotoluene, O$_2$ bubbling (~15 mL/min), 20 °C, UV light irradiation (λ>360 nm). [b] Conversion yield in 2 h, determined by GC-MS analysis, with error ±1%. [c] In this case a selective formation of benzaldehyde (**4a**) and benzoic acid (**4b**) in 65:13 relative yield was observed. [d] At 8 h irradiation time.

To further test the potential of 15% SiW$_{11}$/MES mesoporous for oxidation reactions, various *para*-substituted aryl alcohols, such as 1-phenylethanols (**2** and **3**) and benzyl alcohols (**5** and **6**) were explored. Results, in Table 1 and Fig. S11 of the ESI†, show that these substrates selectively converted to their corresponding ketones (**2a** and **3a**) or aldehydes (**5a** and **6a**) with greater than 93% yield. It is to be noted that 15% SiW$_{11}$/MES achieves quantitative conversion of these alcohols with >99% selectivity in 3 h. As for no-substituted benzyl alcohol (**4**), however, the completive oxidation of **4** towards benzoic acid (**4b**) became remarkable (13% yield of **4b** in 2 h), manifesting a hydrogen atom transfer (HAT) step during the course of reaction.[18] Our catalytic data evidenced also that the presence of

electron-donating or electron-withdrawing groups has a mild effect on the activation of aromatic alcohols. For example, the electron-rich alcohols 1-(*p*-methylphenyl) ethanol (**3**) and *p*-methylbenzyl alcohol (**5**) reacted to form the respective ketone and aldehyde in >94% yield (Table 1). Similar high conversion yields were also observed for electron-deficient 1-(*p*-chlorophenyl)ethanol (**2**) and *p*-chlorobenzyl alcohol (**6**) substrates, though **2** alcohol had slightly slower kinetic (Fig. S12, ESI†). It should be stressed that steric effects of substrate do not significantly affect the transition state of the reaction. For instance, diphenylmethanol (**7**), in which the α-substituent is a phenyl group, reacted about two times faster than **1** and **4** alcohols containing a methyl and hydrogen group next to the benzylic position respectively; k_{Ph}/k_{Me} = 1.9 and k_{Ph}/k_{H} = 2.2. To the best of our knowledge this is the most versatile and active POM-based system thus far developed for photooxidation of aromatic alcohols.[19] Notable, 15% SiW$_{11}$/MES efficiency catalyzed the aerobic oxidation of alicyclic alcohols that are not easily reacted, such as cyclohexanol (**8**) and cyclooctanol (**9**).[20] Thus, **8** and **9** were oxidized to cyclohexanone (**8a**) and cyclooctanone (**9b**) at a 41% and 46% conversion within 8 h irradiation, respectively (Table 1). These results signify the general applicability of the 15% SiW$_{11}$/MES catalyst in the aerobic oxidation of aryl alcohols.

In conclusion, mesoporous POM-based organosilica frameworks with large internal surface area and uniform pores have been successfully prepared though a surfactant-assisted co-polymerization of organically-modified POM clusters ([SiW$_{11}$(SiOH)$_2$]$^{4-}$) with ethane-bridged silsesquioxane linkers. Preliminary photocatalytic studies evidenced that these new hybrid materials are obviously active for photocatalytic aryl alcohol oxidation with molecular oxygen. The synthetic approach using POM clusters as primary building blocks and organo-silsesquioxane linkers will pave the way for the construction of a range of ordered mesoporous solids with designed POM and organic functionality of the pore walls.

Notes and references

Department of Materials Science and Technology, University of Crete, Heraklion 71003, Greece. Tel: +30-2810-545004; Fax: +30-2810-545197; E-mail: garmatas@materials.uoc.gr

† Electronic Supplementary Information (ESI) available: Experimental procedures and additional Tables S1-S2 and Figs. S1-S12. See DOI: 10.1039/c000000x/

1   M.T. Pope and A. Muller, *Polyoxometalate Chemistry: From Topology via Self-Assembly to Applications*, Kluwer, Dordrecht, The Netherlands, 2001.
2   D.E. Katsoulis, *Chem. Rev.*, 1998, **98**, 359; C.L. Hill and M. Prosser-McCartha, *Coord. Chem. Rev.*, 1995, **143**, 407; J. Gao, S. Cao, Q. Tay, Y. Liu, L. Yu, K. Ye, P.C.S. Mun, Y. Li, G. Rakesh, S.C.J. Loo, Z. Chen, Y. Zhao, C. Xue and Q. Zhang, *Sci. Rep.*, 2013, **3**, 1853; B. Hu, C. Wang, J. Wang, J. Gao, K. Wang, J. Wu, G. Zhang, W. Cheng, B. Venkateswarlu, M. Wang, P.S. Lee and Q. Zhang, *Chem. Sci.*, 2014, **5**, 3404.
3   S.L. Suib, *New and Future Developments in Catalysis: Hybrid Materials, Composites, and Organocatalysts*, Elsevier, The Netherlands, 2013, Chap. 13.
4   M. Sugawara, K. Kodato, T. Kuranishi, Y. Nodasaka, K. Sugawara, N. Sakaguchi, T. Nagai, Y. Matsui and W. Ueda, *Angew. Chem. Int. Ed.*, 2008, **47**, 2493; U. Schubert, *Chem. Soc. Rev.*, 2011, **40**, 575.
5   H. Fu, C. Qin, Y. Lu, Z.-M. Zhang, Y.-G. Li, Z.-M. Su, W.-L. Li and E.-B. Wang, *Angew. Chem. Int. Ed.*, 2012, **51**, 7985.

6 S.T. Zheng, J. Zhang and G.-Y. Yang, *Angew. Chem. Int. Ed.*, 2008, **47**, 3909.

7 J. Kang, B. Xu, Z. Peng, X. Zhu, Y. Wei and D.R. Powell, *Angew. Chem. Int. Ed.*, 2005, **44**, 6902; E. Burkholder, V. Colub, C.J. O'Connor and J. Zubieta, *Inorg. Chem.*, 2004, **43**, 7014; C. Streb, C. Ritchie, D.L. Long, P. Kogerler and L. Cronin, *Angew. Chem. Int. Ed.*, 2007, **46**, 7579; P. Mialane, A. Dolbecq and F. Secheresse, *Chem. Commun.*, 2006, 3477; J. Guo, D. Zhang, L. Chen, Y. Song, D. Zhu and Y. Xu, *Dalton Trans.*, 2013, **42**, 8454; S.-T. Zheng, D.-Q. Yuan, H.-P. Jia, J. Zhang and G.-Y. Yang, *Chem. Commun.*, 2007, 1858; D. Dang, Y. Zheng, Y. Bai, X. Guo, P. Ma and J. Niu, *Cryst. Growth Des.*, 2012, **12**, 3856.

8 D. Liu, Y. Lu, H.-Q. Tan, W.-L. Chen, Z.-M. Zhang, Y.-G. Li and E.-B. Wang, *Chem. Commun.*, 2013, **49**, 3673.

9 P.J. Hagrman, D. Hagrman and J. Zubieta, *Angew. Chem. Int. Ed.*, 1999, **38**, 2639; C.J. Brinker and G.W. Scherer, *Sol-Gel Science: The Physics and Chemistry of Sol_Gel Processing*; Academic Press: San Diego, CA, 1990.

10 O.A. Kholdeeva, M.P. Vanina, M.N. Timofeeva, R.I. Maksimovskaya, T.A. Trubitsina, M.S. Melgunov, E.B. Burgina, J. Mrowiec-Bialon and C.L. Hill, *J. Catal.*, 2004, **226**, 363; X.M. Zhang, C. Zhang, H.Q. Guo, W.L. Huang, T. Polenova, L.C. Francesconi and D.L. Akins, *J. Phys. Chem. B*, 2005, **109**, 19156; W. Kaleta, K. Nowinska, *Chem. Comm.*, 2001, 535; S. Polarz, B. Smarsly, C. Goltner and M. Antonietti, *Adv. Mater.*, 2000, **12**, 1503.

11 M.V. Vasylyev and R. Neumann, *J. Am. Chem. Soc.*, 2004, **126**, 884.

12 X. Y. Bao, X. S. Zhao, X. Li, P. A. Chia and J. Li, *J. Phys. Chem. B*, 2004, **108**, 4684; O. Muth, C. Schellbach and M. Fröba, *Chem. Commun.*, 2001, 2032.

13 F. Rouquerol, J. Rouquerol and K. S. W. Sing, *Adsorption by Powders and Porous Solids. Principles, Methodology and Applications*, Academic Press, London, 1999.

14 P. Judeinstein, C. Deprun and L. Nadjo, *J. Chem. Soc., Dalton Trans.*, 1991, 1991.

15 P. H. T. Ngamou, J. P. Overbeek, R. Kreiter, H. M. van Veen, J. F. Vente, I. M. Wienk, P. F. Cuperus and M. Creatore, *J. Mater. Chem. A*, 2013, **1**, 5567.

16 Y. Guo, Y. Yang, C. Hu, C. Guo, E. Wang, Y. Zou and S. Feng, *J. Mater. Chem.*, 2002, **12**, 3046.

17 Assuming that the oxygen concentration remains constant during the reaction, the oxidation of alcohol can be considered a pseudo-first order process, in which the reaction rate is proportional to the concentration of substrate.

18 I. N. Lykakis, M. Orfanopoulos, C. Tanielian, *Org. Lett.,* 2003, **5**, 2875.

19 A. Patel and S, Pathan, *Polyoxomolybdates as Green Catalysts for Aerobic Oxidation*, Springer, Heidelberg, 2014; D. Barats and R. Neumann, *Adv. Synth. Catal.*, 2010, **352**, 293; S. Farhadi and M. Zaidi, *App. Catal. A: Gen.*, 2009, **354**, 119; I. Kornarakis, I.N. Lykakis, N. Vordos and G.S. Armatas, *Nanoscale*, 2014, **6**, 8694.

20 S. Paavola, K. Zetterberg, T. Privalov, I. Csöregh and C. Moberg, *Adv. Synth. Catal.*, 2004, **346**, 237.